Stem Cell Reports
Report

ISSCR

OPEN ACCESS

Efficient Large-Scale 2D Culture System for Human Induced Pluripotent Stem Cells and Differentiated Cardiomyocytes

Shugo Tohyama,[1,2] Jun Fujita,[1,*] Chihana Fujita,[1] Miho Yamaguchi,[1] Sayaka Kanaami,[1] Rei Ohno,[1] Kazuho Sakamoto,[4,6] Masami Kodama,[5] Junko Kurokawa,[6] Hideaki Kanazawa,[1] Tomohisa Seki,[1] Yoshikazu Kishino,[1] Marina Okada,[1] Kazuaki Nakajima,[1] Sho Tanosaki,[1] Shota Someya,[1] Akinori Hirano,[3] Shinji Kawaguchi,[3] Eiji Kobayashi,[2] and Keiichi Fukuda[1]

[1]Department of Cardiology, Keio University School of Medicine, 35 Shinanomachi, Shinjuku-ku, Tokyo 160-8582, Japan
[2]Department of Organ Fabrication, Keio University School of Medicine, 35 Shinanomachi, Shinjuku-ku, Tokyo 160-8582, Japan
[3]Department of Cardiovascular Surgery, Keio University School of Medicine, 35 Shinanomachi, Shinjuku-ku, Tokyo 160-8582, Japan
[4]Department of Pharmacology, Fukushima Medical University School of Medicine, 1 Hikarigaoka, Fukushima 960-1295, Japan
[5]Department of Bio-informational Pharmacology, Medical Research Institute, National University Corporation Tokyo Medical and Dental University, 1-5-45 Yushima, Bunkyo-ku, Tokyo 113-8510, Japan
[6]Department of Bio-Informational Pharmacology, School of Pharmaceutical Sciences, University of Shizuoka, 52-1 Yada, Suruga-ku, Shizuoka 422-8526, Japan
*Correspondence: jfujita@a6.keio.jp
http://dx.doi.org/10.1016/j.stemcr.2017.08.025

SUMMARY

Cardiac regenerative therapies utilizing human induced pluripotent stem cells (hiPSCs) are hampered by ineffective large-scale culture. hiPSCs were cultured in multilayer culture plates (CPs) with active gas ventilation (AGV), resulting in stable proliferation and pluripotency. Seeding of 1×10^6 hiPSCs per layer yielded 7.2×10^8 hiPSCs in 4-layer CPs and 1.7×10^9 hiPSCs in 10-layer CPs with pluripotency. hiPSCs were sequentially differentiated into cardiomyocytes (CMs) in a two-dimensional (2D) differentiation protocol. The efficiency of cardiac differentiation using 10-layer CPs with AGV was 66%–87%. Approximately $6.2–7.0 \times 10^8$ cells (4-layer) and $1.5–2.8 \times 10^9$ cells (10-layer) were obtained with AGV. After metabolic purification with glucose- and glutamine-depleted and lactate-supplemented media, a massive amount of purified CMs was prepared. Here, we present a scalable 2D culture system using multilayer CPs with AGV for hiPSC-derived CMs, which will facilitate clinical applications for severe heart failure in the near future.

INTRODUCTION

Heart failure (HF) causes high mortality and lack of mobility in developed countries. Currently, heart transplantation is the only radical treatment; however, this treatment approach is limited by donor shortages (Lund et al., 2014). Regenerative medicine represents a promising therapeutic alternative for patients with HF. Human induced pluripotent stem cells (hiPSCs) are an ideal cell source and can be acquired from patient tissues (Takahashi et al., 2007). Small amounts of cells (graft size: 1.3×3 mm^2, cell density: 4,500 < viable cells/mm^2 < 29,000) have been used for the treatment of macular degeneration in the first clinical application of hiPSCs (Mandai et al., 2017). However, more than 1×10^9 hiPSC-derived cardiomyocytes (hiPSC-CMs) would be required to recover cardiac function (Kempf et al., 2016).

Although two-dimensional (2D) static culture systems are suitable for both the maintenance and proliferation of hPSCs, most large-scale culture systems for undifferentiated hPSCs have adopted suspension culture systems (SCSs) (Chen et al., 2014; Serra et al., 2012). The biggest advantages of SCSs are easy scale-up of culture volume and effortless medium changes. Undifferentiated hPSCs in SCSs experience shear stress from the agitation, resulting in heterogeneity and differentiation and leading to deterioration of cell quality; thus, optimizing agitation speed is necessary for each cell line (Singh et al., 2010; Zweigerdt et al., 2011). SCSs are more suitable for generation of differentiated cells, as cell aggregation occurs naturally during embryoid body (EB) differentiation (Hemmi et al., 2014; Kempf et al., 2014; Niebruegge et al., 2009). Methods using microcarriers (MCs) in SCSs are another attractive approach for expansion of hPSCs and CMs (Oh et al., 2009). These SCSs have strong advantages in the scale-up of PSCs and CMs. However, complete elimination of the remaining undifferentiated hPSCs in cell aggregates may not be achieved in SCSs, leading to teratoma formation *in vivo* (Hemmi et al., 2014; Hentze et al., 2009).

To eliminate undifferentiated hPSCs from large-scale cultures of hPSC derivatives, Tohyama et al. (2013) developed metabolic purification. Moreover, 2D cell culture is ideal for high-efficiency generation of pure hiPSC-CMs because all cells are evenly exposed to purification medium (Tohyama et al., 2016).

Here, we report a sequential 2D culture system for the generation of large numbers of pure hiPSC-CMs with high efficiency.

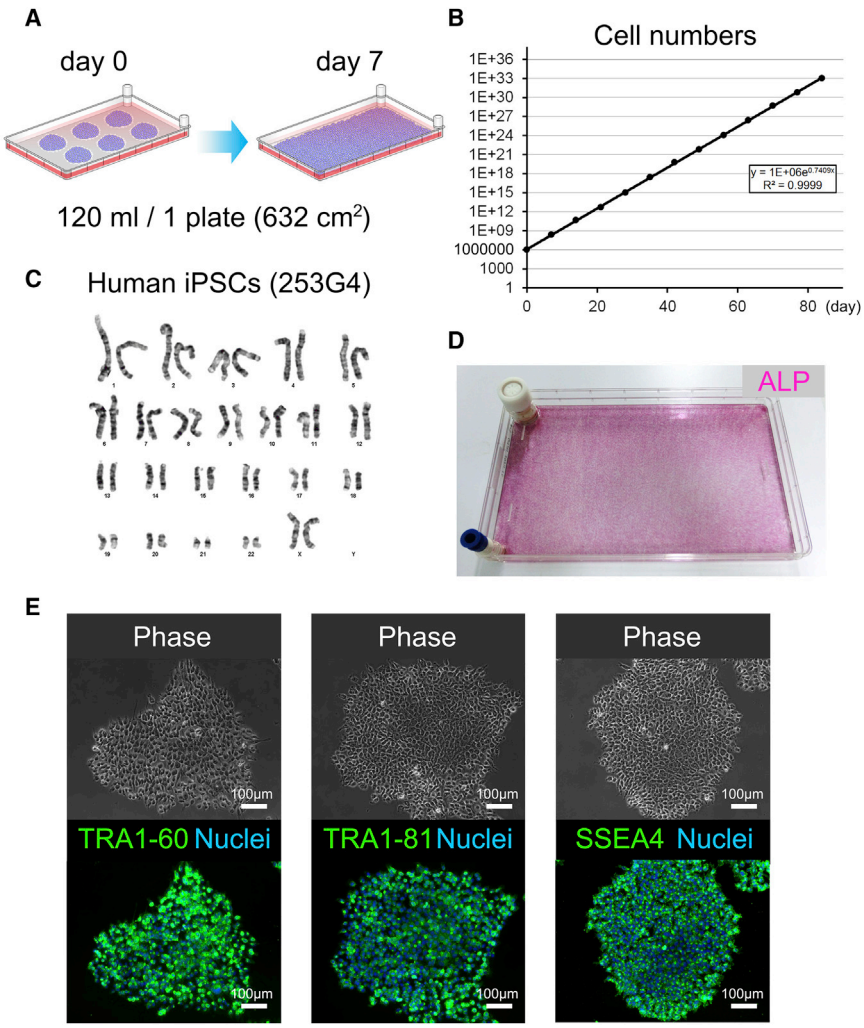

Figure 1. hiPSCs Were Cultured in a Single-Layer CP

(A) Schematic representation of the cell culture in a single-layer CP; the total volume of cells in each plate was 120 mL.

(B) Growth curve of hiPSCs (253G4) in a single-layer CP. Each dot represents a passage of cells.

(C) Karyotype of hiPSCs (253G4) after cell culture in a single-layer CP.

(D) Maintenance of hiPSCs (253G4) in the undifferentiated state as determined by alkaline phosphatase staining.

(E) hiPSC (253G4) expression of the pluripotency markers TRA1-60, TRA1-81, and SSEA4. Scale bars represent 100 μm.

See also Figure S1.

RESULTS

Expansion of hiPSCs in a Single-Layer Culture Plate

We evaluated a large-scale 2D culture system with multilayer culture plates (CPs) and active gas ventilation (AGV) for production of hiPSCs and differentiated CMs. First, hiPSCs (253G4) were passaged in a single-layer CP in a normal gas incubator for 7 days as controls (Figure 1A). The culture area of the plate was 632 cm^2, which is more than 11-fold larger than that of a 10-cm dish (55 cm^2). The proliferation rate was approximately 187-fold (Figure 1B). Upon inoculation of 1×10^6 hiPSCs, approximately 1.9×10^8 hiPSCs were consistently obtained from a confluent single-layer CP over a 7-day period (3.0×10^5 cells/cm^2). The karyotype of the cultured hiPSCs was normal (Figure 1C). The pluripotent state was verified by alkaline phosphatase (AP) staining. All colonies were AP positive, and hiPSCs were evenly cultured throughout the single-layer CP (Figure 1D). Immunofluorescence staining additionally confirmed strong expression of pluripotency markers in all colonies (Figure 1E). These data strongly indicated that the present large-scale 2D culture system was suitable for the maintenance of pluripotency in hiPSCs.

Expansion of hiPSCs in a Multilayer CP with or without AGV

Next, hiPSCs (253G4) were cultured in 4-layer CPs with AGV (Figure S1A). The AGV system enabled the maintenance of 5% carbon dioxide (CO_2) in every layer of a 4- or 10-layer CP. When 4×10^6 hiPSCs were seeded in a 4-layer CP, the number of hiPSCs increased by 179-fold over a 7-day period (Figure S1B). The proliferation efficiency in a 4-layer CP with AGV was almost equal to that of a single-layer CP (Figure S1C). Pluripotency was also confirmed by immunofluorescence staining of NANOG, OCT4, TRA1-60, and SSEA4 (Figure S1D). To evaluate the differences between AGV and normal gas

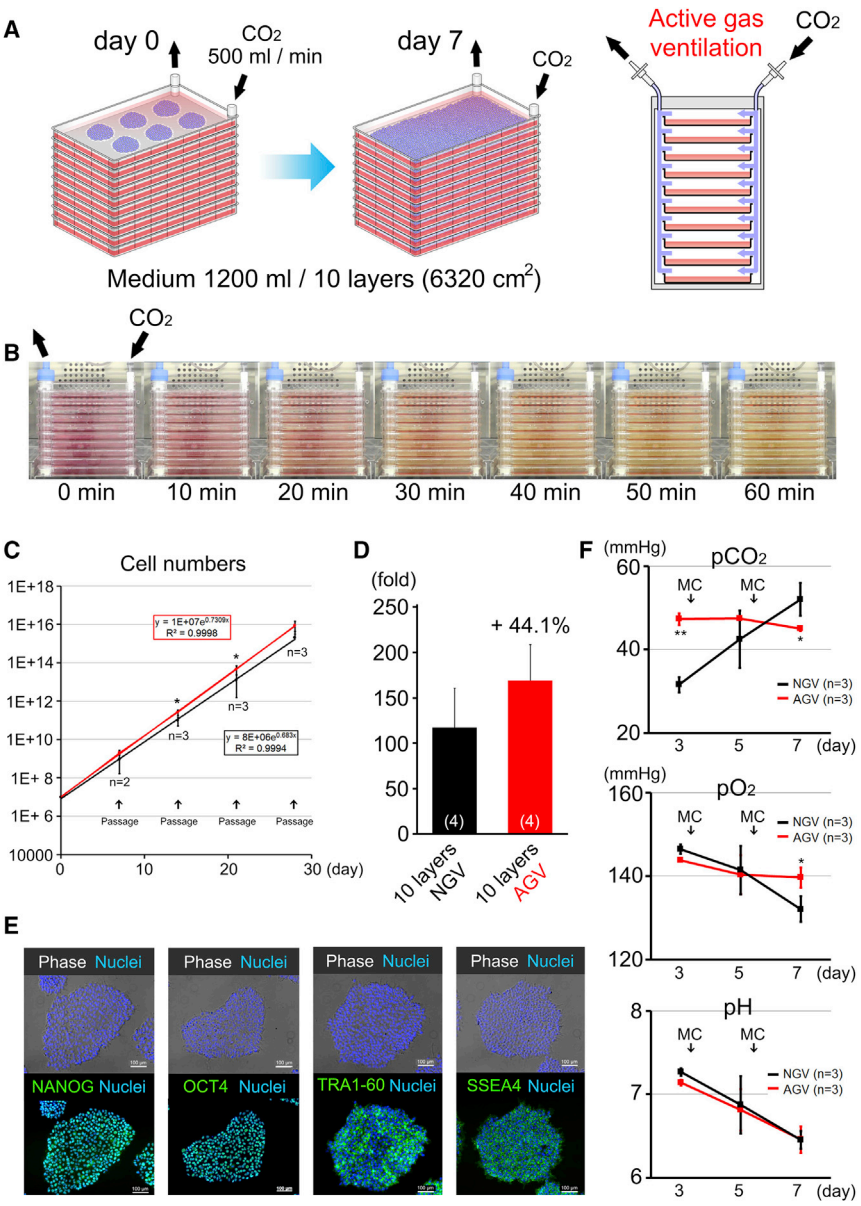

Figure 2. The 10-Layer CP System Was Useful for Acquisition of Large Numbers of hiPSCs

(A) Schematic representation of cell culture in a 10-layer CP under active gas ventilation (AGV); the total volume of medium was 1,200 mL per 10-layer CP.

(B) Rapid conversion of phenol red in the PBS from red to yellow color over a 1-hr period in the AGV system.

(C) Growth curves of hiPSCs (253G4) in a 10-layer CP under normal gas ventilation (NGV, black) or AGV (red). Each dot represents the average cumulative cell numbers in each passage.

(D) Proliferation rates in 10-layer CPs under NGV (n = 4) or AGV (n = 4). Each bar represents the average of the fold changes from individual passages.

(E) hiPSC (253G4) expression of the pluripotency markers NANOG, OCT4, TRA1-60, and SSEA4, as determined by immunofluorescence staining. Scale bars represent 100 μm.

(F) pCO_2, pO_2, and pH levels during cultivation in a 10-layer CP under NGV or AGV (n = 3 independent experiments).

Data are presented as mean ± SD. *p < 0.05; **p < 0.01. See also Figure S2.

ventilation (NGV), we measured the bioprofiles (partial pressure of CO_2 [pCO_2], partial pressure of O_2 [pO_2], pH, glucose, and glutamine) in the culture medium in 4-layer CPs under AGV or NGV (Figure S1E). pCO_2 was stable at each time point under AGV; however, it significantly increased with time under NGV. pH decreased under both conditions. pO_2 was not significantly changed, whereas glucose and glutamine remarkably decreased in hiPSC cultures over time, as reported previously (Tohyama et al., 2013, 2016).

Finally, hiPSCs (253G4) were cultured in 10-layer CPs with AGV (Figure 2A). First, we examined the feasibility of 10-layer CPs with the AGV system. To examine the permeation of CO_2 in each layer, we observed changes in phenol red color in medium over time. Phenol red in PBS rapidly turned from red to yellow after 1 hr in the AGV system (Figure 2B). Next, the gas exchange rate was examined using nitrogen filling. The exchange of air was almost completed in 4 hr using the AGV system (Figure S2A). However, gas exchange could not be completed using the NGV system, even over a 24-hr period (Figure S2B). The proliferation efficiency was also compared between NGV and AGV incubators. The proliferation of hiPSCs with AGV was more stable than that with NGV (Figure 2C). With AGV, the yield was 1.7×10^9 hiPSCs (44% more than under NGV conditions) in the 10-layer CPs over a 7-day period (Figure 2D).

Furthermore, the morphology of hiPSCs was normal, and cells were clearly stained with OCT4, NANOG, SSEA4, and TRA1-60 (Figure 2E). The expression of pluripotent markers was also confirmed by flow-cytometry analysis (Figure S2C). The differences between AGV and NGV in 10-layer CPs were also compared using bioprofiles (Figure 2F). Even in the 10-layer CPs, pCO_2 was more stable at each time point under AGV; however, it was much lower at day 3 and significantly increased with time under NGV. pH decreased under both conditions in the same way as it did in the 4-layer CPs. Unlike in the 4-layer CPs, pO_2 significantly decreased under NGV conditions. Bioprofiles in 10-cm dishes confirmed that pCO_2 in multilayer CPs under AGV was as stable as in ordinary cell culture. Moreover, pO_2 was more stable in multilayer CPs (Figures 2F and S2D). These results indicated that AGV was necessary to culture hiPSCs efficiently in multilayer CPs.

Cardiac Differentiation from hiPSCs in a Multilayer CP with or without AGV

hiPSCs (253G4, 201B7, and FfI14) were sequentially differentiated into CMs from 90% confluent hiPSCs in 4- or 10-layer CPs (Figure 3A). The hiPSC-CMs started to beat at 7–10 days. Cells were collected at day 10 and analyzed by immunofluorescence staining and flow cytometry. Cell viabilities after cardiac differentiation in single-, 4-, or 10-layer CPs under NGV or AGV were over 95% (Figure 3B). Total cell numbers after differentiation derived from hiPSCs (253G4) in single-, 4-, or 10-layer CPs under AGV were 1.5×10^8, 6.7×10^8, and 1.5×10^9, respectively (Figures 3C, S3A, and S3B). Total cell number after differentiation derived from other cell lines (201B7 and FfI14) in a 4-layer CP was $6.2–7.0 \times 10^8$ (Figure S3B). The cardiac differentiation efficiency (253G4 and FfI14) was not significantly different in 10-layer CPs between AGV and NGV (Figures 3D and S3C). In contrast, total hiPSC-CM numbers were higher in AGV than in NGV because proliferative efficiency in lower chambers of 10-layer CPs was low (Figures 3D, S3C, and S3D). The proportion of cardiac troponin T (cTnT)-positive cells derived from hiPSCs (253G4) using 10-layer CPs was approximately 80% (Figure 3E). The differentiated CMs were then enzymatically dissociated and seeded on single-layer CPs or 15-cm dishes. Next, the cells were metabolically selected under glucose- and glutamine-depleted and lactate-supplemented conditions (Tohyama et al., 2016). Expression of the cardiac marker α-actinin was confirmed by immunofluorescence staining (Figures 3F, 3G, and S3E). Flow-cytometry analysis confirmed that following this metabolic selection, almost all cells (>97%) clearly expressed cTnT (Figures 3H, S3F, and S3G; Movie S1). The yield-based efficiency by metabolic selection was 77.5% (Figure S3H), and the viability of the cryopreserved cells after thawing was over 80% (Figure S3I).

Characterization of Metabolically Purified hiPSC-CMs

The characteristics of pure hiPSC-CMs via cryopreservation were analyzed by immunostaining. Most hiPSC-CMs developed into the myosin light chain 2v (MLC2v)-positive ventricular phenotype after metabolic selection (Figure 4A). Electrophysiological characteristics of pure hiPSC-CMs were analyzed by the whole-cell patch-clamp technique and multielectrode array system. The typical action potential of ventricular CMs was recorded, and the results of maximum diastolic potential, action potential amplitude, and action potential duration at 50% of the amplitude supported the ventricular phenotype of pure hiPSC-CMs (Figures 4B and 4C). To assess functional properties, we added isoproterenol to stimulate β-adrenoceptor (Figure 4B). The beating rate increased in a concentration-dependent manner (Figures 4D and 4E). Addition of E-4031 (a water-soluble hERG channel blocker) to pure hiPSC-CMs prolonged field potential duration, a surrogate marker for QT-interval (Figures 4F and 4G). These data confirmed that pure hiPSC-CMs via cryopreservation had normal electrophysiological properties.

DISCUSSION

A serial large-scale cell culture system using multilayer CPs with AGV was established for hiPSCs and differentiated CMs. A clinically necessary number of hiPSC-CMs was efficiently obtained from both 4- and 10-layer CPs. Finally, the cells were refined by metabolic selection.

Although the cardiac differentiation protocol was reformed, the cardiac differentiation efficiency from hiPSCs depends on the cell line, and such procedures often produce hiPSC-CMs with low efficiency (Mummery et al., 2012). Moreover, hiPSC-CMs exhibit a fetal phenotype and gradually lose proliferative capacity after cardiac differentiation over time (Zhang et al., 2009). Therefore, the large number of hiPSCs present is a major premise for obtaining hiPSC-CMs on a large scale.

In previous studies, 2D monolayer culture was established as a conventional culture system for undifferentiated hPSCs (Takahashi et al., 2007; Thomson et al., 1998). This standard culture method has the advantage of maintaining the pluripotent state and high differentiation potential. Moreover, 2D monolayer culture is also advantageous for cardiac differentiation because all cells are uniformly exposed to medium, including growth factors, small molecules, and paracrine factors (Lian et al., 2013; Mummery et al., 2012). The main disadvantage of 2D culture systems is low cell yield due to the limited surface area. Thus, 2D culture systems usually need "scale out" to acquire large amounts of cells; this necessitates substantial space and labor (Kempf et al., 2016). Multilayer CPs overcame these

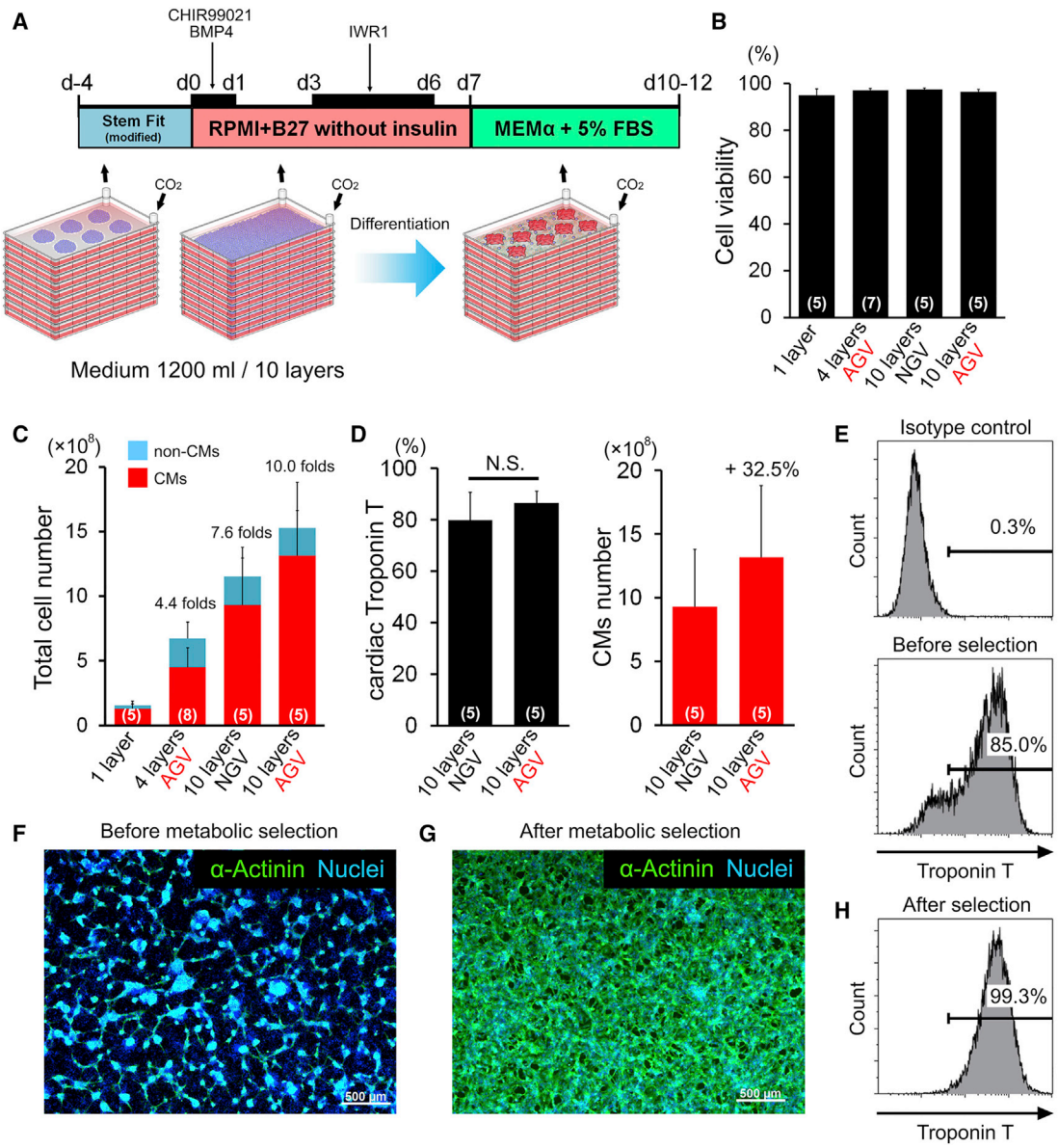

Figure 3. Large-Scale Culture of Cardiac Differentiation from hiPSCs in a Multilayer CP

(A) Schematic representation of the cardiac differentiation protocol. The expanded hiPSCs were successively cultured for cardiac differentiation in 4- or 10-layer CPs. d, day; FBS, fetal bovine serum.

(B) The bar graphs show cell viability after cardiac differentiation from hiPSCs (253G4) in single-layer (n = 5), 4-layer (n = 7), or 10-layer (n = 5) CPs under NGV or AGV. Data were obtained from independent experiments.

(C) Total cell number of hiPSC (253G4)-derived cells in single-layer (n = 5), 4-layer (n = 8), or 10-layer (n = 5) CPs under NGV or AGV. Data were obtained from independent experiments.

(D) The proportion and final yield of troponin T-positive cardiomyocytes (CMs) derived from hiPSCs (253G4) in 10-layer CPs under NGV or AGV (n = 5 independent experiments). N.S., not significant.

(E) Representative flow-cytometry analysis for troponin T-positive cells in 10-layer CPs under AGV.

(F and G) Representative immunofluorescence staining for α-actinin (green) and nuclei (blue) in hiPSC (253G4)-derived dispersed cells before (F) and after (G) metabolic selection. Scale bars represent 500 μm.

(H) Representative flow-cytometry analysis for troponin T-positive cells after metabolic selection.

Data are presented as mean ± SD. See also Figure S3.

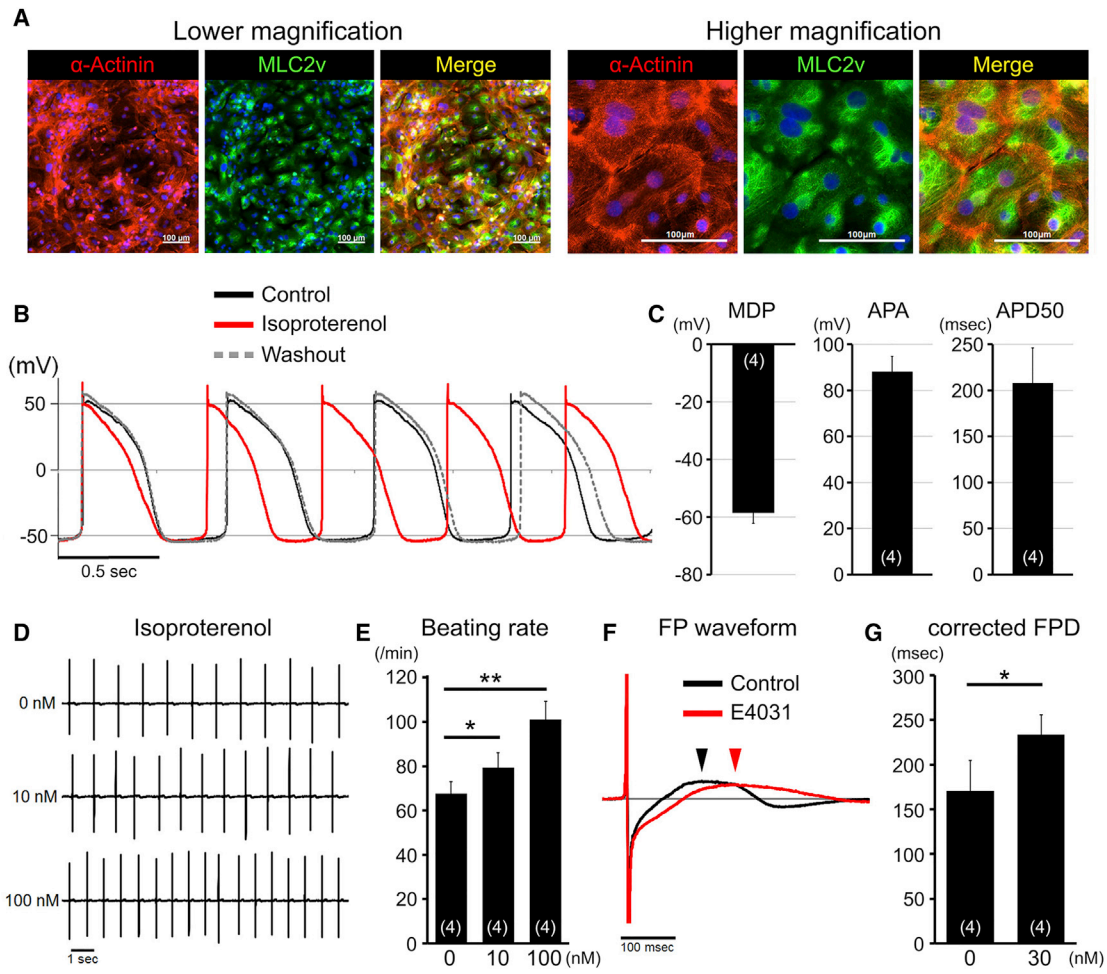

Figure 4. Electrophysiological Properties of Purified hiPSC-CMs

(A) Immunofluorescence staining for α-actinin (red), MLC2v (green), and nuclei (blue) in purified hiPSC (253G4)-CMs after thawing. Scale bars represent 100 μm.

(B) Metabolically purified CMs after thawing showed ventricular-like action potentials (n = 4 independent experiments) and responded to isoproterenol (10 nM) administration.

(C) The bar graphs show maximum diastolic potential (MDP), action potential amplitude (APA), and action potential duration at 50% of the amplitude (APD50) in metabolically purified CM after thawing (n = 4 independent experiments). Data are presented as mean ± SEM.

(D) Representative field potentials (FPs) in metabolically purified CMs with or without isoproterenol administration.

(E) The graph summarizes changes in beating rates with or without isoproterenol administration (n = 4 independent experiments). Data are presented as mean ± SD.

(F) Representative FPs in metabolically purified CM with or without E4031 administration.

(G) The graph summarizes changes in corrected field potential duration (FPD) with or without E4031 administration (n = 4 independent experiments). Data are presented as mean ± SD.

*p < 0.05; **p < 0.01.

problems (Schulz et al., 2012), but it was difficult to maintain the CO_2 concentration in each layer evenly in NGV. Fluctuation of CO_2 concentration could affect cell behavior; highly elevated CO_2 levels cause mitochondrial dysfunction and impair cell proliferation regardless of acidosis (Vohwinkel et al., 2011). Recently, it was reported that mitochondrial oxidative phosphorylation played an important role in survival and proliferation of hiPSCs as well as hiPSC-CMs (Tohyama et al., 2016). Therefore, one reason for the efficient culture of hiPSCs and hiPSC-CMs that we observed using multilayer CPs may be the stable maintenance of pO_2 and pCO_2 allowed by AGV.

Other disadvantages of the 2D culture system are cell harvesting and the lack of control of important culture parameters. Cell harvesting is relatively difficult from multilayer CPs in comparison with single-layer CPs. In our

experiments, hiPSC recovery from 4-layer CPs was almost same as that of hiPSCs from single-layer CPs (Figure S1C). However, cell recovery in 10-layer CPs with AGV was estimated to be approximately 90% (Figures S1C and 2D). The total cell yield of 10-layer CPs outweighed this cell loss; however, this problem should be addressed in future studies to improve efficiency. Monitoring of culture conditions is also necessary in future studies of large-scale 2D culture systems using multilayer CPs.

The scalable culture system for hPSCs was mainly researched using SCSs (Chen et al., 2014; Krawetz et al., 2010; Silva et al., 2015). The shear stress caused by agitation can affect both pluripotency of hiPSCs and differentiation potential. If spheroid-formed hPSCs in SCSs are not maintained appropriately, they are at high risk of losing pluripotency and developing into EBs (Krawetz et al., 2010; Singh et al., 2010). Particularly with regard to clinical applications, it would be difficult to evaluate the undifferentiated state by observation of hiPSC morphology.

SCSs for somatic differentiation were more common in hPSC culture and were also effective for cardiac development (Hemmi et al., 2014; Kempf et al., 2014; Niebruegge et al., 2009). When stirred conditions (agitation speed, impeller type, cell density) are appropriately adjusted, cells are easily scaled up, and culture conditions can be monitored with a bioreactor (Kempf et al., 2014; Olmer et al., 2012). However, there is a high possibility that residual undifferentiated hPSCs exist in the EBs. We developed a metabolic selection system with glucose- and glutamine-depleted as well as lactate-supplemented conditions for expansion of clinical-grade hiPSC-CMs (Tohyama et al., 2016). For clinical applications, the remaining hPSCs in EBs are much more difficult to completely eliminate during purification because they stick to each other, and the purification medium may not reach the cells on the inside of the clumps. If cell aggregates are forced to dissociate, they lose the viability. In contrast, cardiac differentiation in 2D culture was efficient and made it easier to observe cellular status and achieve purification.

MCs are another unique large-scale culture system providing sufficient surface area for cell adhesion in SCSs. MCs were used in static conditions and applied to stirred SCSs (Oh et al., 2009). Recently, serum-free and xeno-free SCSs with MCs also became available (Badenes et al., 2016a; Lam et al., 2014a). Despite using MCs, some PSC lines exhibit unavoidable shear stress in stirred SCSs (Leung et al., 2011). Lower shear stress results in highly efficient cardiac differentiation (Ting et al., 2014). MC type, aggregation size, and MC coating are also important for scalable expansion and controlled differentiation of hPSCs (Lam et al., 2014b; Lecina et al., 2010). Cost-effective, xeno-free, and synthetic, dissolvable MCs using non-proteolytic enzymes must be developed for clinical translation (Badenes et al., 2016b; Chen et al., 2014).

In summary, an efficient scalable 2D culture system was developed for the serial culture of undifferentiated hiPSCs until cardiac differentiation. Furthermore, the metabolic selection system enabled successful purification of the expanded hiPSC-CMs. This innovative massive culture system will be useful for generating a large number of hiPSC-CMs with high efficiency for clinical applications.

EXPERIMENTAL PROCEDURES

Measurement of pCO_2, pO_2, pH, and Metabolites in Culture Medium

Under AGV and NGV, pCO_2, pO_2, pH, glucose, and glutamine levels in the medium were measured using a BioProfile 400 Analyzer (Nova Biomedical, USA) during the maintenance and cultivation of hiPSCs using the multilayer CPs or 10-cm culture dishes.

SUPPLEMENTAL INFORMATION

Supplemental Information includes Supplemental Experimental Procedures, three figures, and one movie and can be found with this article online at http://dx.doi.org/10.1016/j.stemcr.2017.08.025.

AUTHOR CONTRIBUTIONS

S. Tohyama and J.F. conceived the study; S. Tohyama, C.F., M.Y., S. Kanaami, and R.O. performed the experiments; K.S., M.K., and J.K. performed the electrophysiological experiments; S. Tohyama, J.F., H.K., T.S., Y.K., and M.O. analyzed the data; S. Tanosaki and S.S. designed the methodology; K.N., A.H., and S. Kawaguchi contributed to specific experiments; J.F. and S. Tohyama wrote the manuscript; J.F., E.K., and K.F. supervised the study.

ACKNOWLEDGMENTS

The authors thank the Center for iPSC Research and Application, Kyoto University, for providing the 253G4, 201B7, and Ff114 hiPSC lines. This work was supported by the Highway Program for Realization of Regenerative Medicine from the Japan Science and Technology Agency (no. 16bm0504006h0006 to K.F.) and partly supported by the Support Program to Break the Bottlenecksat R&D for Accelerating the Practical Use of Health Research Outcomes (no. 34201006-01 to K.F.), a Japan Society for the Promotion of Science JSPS KAKENHI grant (no. 16K09507 to J.F., no. 15H04684 to J.K., and no. 15K09098 to H.K.), and the SENSHIN Medical Research Foundation (to S. Tohyama). The authors are grateful to Satoru Okamoto, Yusuke Natsume, and Kotoe Terasawa for providing the medium (Ajinomoto Co., Inc.) and to Yoshihide Miyatani and Akira Yamamoto for adjusting the incubators with the AGV system (Taitec Corporation). K.F., who is a co-founder of Heartseed, Inc., has equity in Heartseed, Inc.

Received: December 11, 2016
Revised: August 30, 2017
Accepted: August 31, 2017
Published: October 5, 2017

REFERENCES

Badenes, S.M., Fernandes, T.G., Cordeiro, C.S., Boucher, S., Kuninger, D., Vemuri, M.C., Diogo, M.M., and Cabral, J.M. (2016a). Defined essential 8 medium and vitronectin efficiently support scalable xeno-free expansion of human induced pluripotent stem cells in stirred microcarrier culture systems. PLoS One *11*, e0151264.

Badenes, S.M., Fernandes, T.G., Rodrigues, C.A., Diogo, M.M., and Cabral, J.M. (2016b). Microcarrier-based platforms for in vitro expansion and differentiation of human pluripotent stem cells in bioreactor culture systems. J. Biotechnol. *234*, 71–82.

Chen, K.G., Mallon, B.S., McKay, R.D., and Robey, P.G. (2014). Human pluripotent stem cell culture: considerations for maintenance, expansion, and therapeutics. Cell Stem Cell *14*, 13–26.

Hemmi, N., Tohyama, S., Nakajima, K., Kanazawa, H., Suzuki, T., Hattori, F., Seki, T., Kishino, Y., Hirano, A., Okada, M., et al. (2014). A massive suspension culture system with metabolic purification for human pluripotent stem cell-derived cardiomyocytes. Stem Cells Transl. Med. *3*, 1473–1483.

Hentze, H., Soong, P.L., Wang, S.T., Phillips, B.W., Putti, T.C., and Dunn, N.R. (2009). Teratoma formation by human embryonic stem cells: evaluation of essential parameters for future safety studies. Stem Cell Res. *2*, 198–210.

Kempf, H., Andree, B., and Zweigerdt, R. (2016). Large-scale production of human pluripotent stem cell derived cardiomyocytes. Adv. Drug Deliv. Rev. *96*, 18–30.

Kempf, H., Olmer, R., Kropp, C., Ruckert, M., Jara-Avaca, M., Robles-Diaz, D., Franke, A., Elliott, D.A., Wojciechowski, D., Fischer, M., et al. (2014). Controlling expansion and cardiomyogenic differentiation of human pluripotent stem cells in scalable suspension culture. Stem Cell Reports *3*, 1132–1146.

Krawetz, R., Taiani, J.T., Liu, S., Meng, G., Li, X., Kallos, M.S., and Rancourt, D.E. (2010). Large-scale expansion of pluripotent human embryonic stem cells in stirred-suspension bioreactors. Tissue Eng. Part C Methods *16*, 573–582.

Lam, A.T., Chen, A.K., Li, J., Birch, W.R., Reuveny, S., and Oh, S.K. (2014a). Conjoint propagation and differentiation of human embryonic stem cells to cardiomyocytes in a defined microcarrier spinner culture. Stem Cell Res. Ther. *5*, 110.

Lam, A.T., Li, J., Chen, A.K., Reuveny, S., Oh, S.K., and Birch, W.R. (2014b). Cationic surface charge combined with either vitronectin or laminin dictates the evolution of human embryonic stem cells/microcarrier aggregates and cell growth in agitated cultures. Stem Cells Dev. *23*, 1688–1703.

Lecina, M., Ting, S., Choo, A., Reuveny, S., and Oh, S. (2010). Scalable platform for human embryonic stem cell differentiation to cardiomyocytes in suspended microcarrier cultures. Tissue Eng. Part C Methods *16*, 1609–1619.

Leung, H.W., Chen, A., Choo, A.B., Reuveny, S., and Oh, S.K. (2011). Agitation can induce differentiation of human pluripotent stem cells in microcarrier cultures. Tissue Eng. Part C Methods *17*, 165–172.

Lian, X., Zhang, J., Azarin, S.M., Zhu, K., Hazeltine, L.B., Bao, X., Hsiao, C., Kamp, T.J., and Palecek, S.P. (2013). Directed cardiomyocyte differentiation from human pluripotent stem cells by modulating Wnt/beta-catenin signaling under fully defined conditions. Nat. Protoc. *8*, 162–175.

Lund, L.H., Edwards, L.B., Kucheryavaya, A.Y., Benden, C., Christie, J.D., Dipchand, A.I., Dobbels, F., Goldfarb, S.B., Levvey, B.J., Meiser, B., et al. (2014). The registry of the International Society for Heart and Lung Transplantation: thirty-first official adult heart transplant report—2014; focus theme: retransplantation. J. Heart Lung Transplant. *33*, 996–1008.

Mandai, M., Watanabe, A., Kurimoto, Y., Hirami, Y., Morinaga, C., Daimon, T., Fujihara, M., Akimaru, H., Sakai, N., Shibata, Y., et al. (2017). Autologous induced stem-cell-derived retinal cells for macular degeneration. N. Engl. J. Med. *376*, 1038–1046.

Mummery, C.L., Zhang, J., Ng, E.S., Elliott, D.A., Elefanty, A.G., and Kamp, T.J. (2012). Differentiation of human embryonic stem cells and induced pluripotent stem cells to cardiomyocytes: a methods overview. Circ. Res. *111*, 344–358.

Niebruegge, S., Bauwens, C.L., Peerani, R., Thavandiran, N., Masse, S., Sevaptisidis, E., Nanthakumar, K., Woodhouse, K., Husain, M., Kumacheva, E., et al. (2009). Generation of human embryonic stem cell-derived mesoderm and cardiac cells using size-specified aggregates in an oxygen-controlled bioreactor. Biotechnol. Bioeng. *102*, 493–507.

Oh, S.K., Chen, A.K., Mok, Y., Chen, X., Lim, U.M., Chin, A., Choo, A.B., and Reuveny, S. (2009). Long-term microcarrier suspension cultures of human embryonic stem cells. Stem Cell Res. *2*, 219–230.

Olmer, R., Lange, A., Selzer, S., Kasper, C., Haverich, A., Martin, U., and Zweigerdt, R. (2012). Suspension culture of human pluripotent stem cells in controlled, stirred bioreactors. Tissue Eng. Part C Methods *18*, 772–784.

Schulz, T.C., Young, H.Y., Agulnick, A.D., Babin, M.J., Baetge, E.E., Bang, A.G., Bhoumik, A., Cepa, I., Cesario, R.M., Haakmeester, C., et al. (2012). A scalable system for production of functional pancreatic progenitors from human embryonic stem cells. PLoS One *7*, e37004.

Serra, M., Brito, C., Correia, C., and Alves, P.M. (2012). Process engineering of human pluripotent stem cells for clinical application. Trends Biotechnol. *30*, 350–359.

Silva, M.M., Rodrigues, A.F., Correia, C., Sousa, M.F., Brito, C., Coroadinha, A.S., Serra, M., and Alves, P.M. (2015). Robust expansion of human pluripotent stem cells: integration of bioprocess design with transcriptomic and metabolomic characterization. Stem Cells Transl. Med. *4*, 731–742.

Singh, H., Mok, P., Balakrishnan, T., Rahmat, S.N., and Zweigerdt, R. (2010). Up-scaling single cell-inoculated suspension culture of human embryonic stem cells. Stem Cell Res. *4*, 165–179.

Takahashi, K., Tanabe, K., Ohnuki, M., Narita, M., Ichisaka, T., Tomoda, K., and Yamanaka, S. (2007). Induction of pluripotent stem cells from adult human fibroblasts by defined factors. Cell *131*, 861–872.

Thomson, J.A., Itskovitz-Eldor, J., Shapiro, S.S., Waknitz, M.A., Swiergiel, J.J., Marshall, V.S., and Jones, J.M. (1998). Embryonic

stem cell lines derived from human blastocysts. Science *282*, 1145–1147.

Ting, S., Chen, A., Reuveny, S., and Oh, S. (2014). An intermittent rocking platform for integrated expansion and differentiation of human pluripotent stem cells to cardiomyocytes in suspended microcarrier cultures. Stem Cell Res. *13*, 202–213.

Tohyama, S., Fujita, J., Hishiki, T., Matsuura, T., Hattori, F., Ohno, R., Kanazawa, H., Seki, T., Nakajima, K., Kishino, Y., et al. (2016). Glutamine oxidation is indispensable for survival of human pluripotent stem cells. Cell Metab. *23*, 663–674.

Tohyama, S., Hattori, F., Sano, M., Hishiki, T., Nagahata, Y., Matsuura, T., Hashimoto, H., Suzuki, T., Yamashita, H., Satoh, Y., et al. (2013). Distinct metabolic flow enables large-scale purification of mouse and human pluripotent stem cell-derived cardiomyocytes. Cell Stem Cell *12*, 127–137.

Vohwinkel, C.U., Lecuona, E., Sun, H., Sommer, N., Vadasz, I., Chandel, N.S., and Sznajder, J.I. (2011). Elevated CO(2) levels cause mitochondrial dysfunction and impair cell proliferation. J. Biol. Chem. *286*, 37067–37076.

Zhang, J., Wilson, G.F., Soerens, A.G., Koonce, C.H., Yu, J., Palecek, S.P., Thomson, J.A., and Kamp, T.J. (2009). Functional cardiomyocytes derived from human induced pluripotent stem cells. Circ. Res. *104*, e30–e41.

Zweigerdt, R., Olmer, R., Singh, H., Haverich, A., and Martin, U. (2011). Scalable expansion of human pluripotent stem cells in suspension culture. Nat. Protoc. *6*, 689–700.